

Sizes and polycyclic aromatic hydrocarbon composition distributions of nano, ultrafine, fine, and coarse particulates emitted from a four-stroke motorcycle

SHU M. CHIEN and YUH J. HUANG

Department of Biomedical Engineering & Environmental Sciences, National Tsing Hua University, Hsinchu, Taiwan

Thus, this study was undertaken to determine the size distribution, concentration, species, and carcinogenic potency of particulate matter and particle-bound polycyclic aromatic hydrocarbons (PAHs) emitted from 4-st/mc at various speeds (idle, 15 km/h, 30 km/h). Approximately 80% of the particles emitted from the that is, they are primary inhalable particulates. The particle total number concentrations (TNCs) emitted while idling and at 15 and 30 km/h were 2.07×10^4 , 2.35×10^4 , and 2.60×10^4 #/cm³, respectively; i.e., they increased at elevated speeds. Notably, most of the particles emitted at 30 km/h had diameters of less than 0.65 μm and contained higher percentages of total PAHs. Excluding incomplete combustion, we suspected that some of the lower-molecular-weight PAHs [phenanthrene (PA), anthracene (Ant), pyrene (Pyr)] obtained in the fine particles at idle originated from unburned 95-octane unleaded fuel. When operated at 15 km/h, pyrolysis of the PAHs dominated, resulting in increased amounts of medium-molecular-weight PAHs {fluorene (FL), Pyr, benz[a]anthracene (BaA), chrysene (CHR)} in the ultrafine particles. Furthermore, at 30 km/h, more pyrosynthesis products {benzo[a]pyrene (BaP), indeno[1,2,3,-cd]pyrene (IND), dibenz[a,h]anthracene (DBA)}, induced through combustion at the correspondingly higher temperature, were exhausted with the nanoparticles. Although the total concentrations of BaP-equivalent emissions were inconsistent with the total PAHs, the nanoscale-sized particulates emitted from the 4-st/mc at higher speeds had the strongest PAH-related carcinogenic potencies, which should be a great concern.

Keywords: Four-stroke motorcycle, PAHs, carcinogenicity, electrical low pressure impactor (ELPI).

Introduction

The high mobility, convenience, and low fuel consumption of motorcycles makes them attractive on-road vehicles in both the urban and suburban areas of many tropical and subtropical countries. In Taiwan, for example, there are over 13.2×10^6 motorcycles, accounting for 67% of all motor vehicles; in addition, the number of motorcycles per area is among the highest in the world (315 motorcycles/km²).^[1] Two- and four-stroke motorcycles comprise ca. 35 and 65%, respectively, of the motorcycles in Taiwan. Although many studies have been conducted to measure the levels of regulated air pollutants, such as carbon monoxide (CO), hydrocarbons (HCs), and nitrogen oxide (NO_x), released from motorcycles,^[2–4] the levels of several unregulated constituents, especially combined with

particulate matter (PM), might be of greater concern for their potential health effects.

Atmospheric PM contains various carcinogenic and mutagenic compounds that are generally accepted to cause respiratory diseases, such as lung cancer. Polycyclic aromatic hydrocarbons (PAHs) are typical indirect- and direct-acting mutagenic compounds.^[5,6] Motor vehicles are major sources of PAH emissions.^[7–9] PAHs are formed as a complex mixture of compounds during the incomplete combustion of organic matter. Most carcinogenic PAHs are associated with particulates-predominantly, fine particulates.^[6,10] The particle number concentrations and size distributions of these mutagenic compounds are two of the major factors used to assess their influence on human health: the particle size controls the deposition behavior of PMs in respiratory organs and the number concentration affects the carcinogenic rate.

The particle size distributions of PAHs emitted from two-stroke motorcycles (2-st/mcs) have been studied previously.^[11] In general, 2-stk/mcs are often run using a mixture of gasoline and a lubricant, causing the emission of unburned oil.^[12] The exhaust emitted from a 2-stk/mc contains more regulated air pollutants^[2,13–15] and PAHs^[3,16]

Address correspondence to Yuh-Jeen Huang, Department of Biomedical Engineering & Environmental Sciences, National Tsing Hua University, Hsinchu, Taiwan 30013, R. O. C.; E-mail: yjhuang@mx.nthu.edu.tw
Received April 12, 2010.

than that from a 4-st/mc. Nevertheless, 4-st/mcs are becoming increasingly popular in many countries. Therefore, to provide an advanced health risk assessment, we aimed to characterize the particulate and particle size distributions of PAHs in the exhaust from a 4-st/mc.

The cascade impactor approach has been used previously to investigate the particle size distributions of PAHs emitted from diesel and gasoline vehicles.^[17–21] In this study, particle-bound PAHs in the 4-st/mc exhaust were size-segregated, from 0.03 to 10 μm , using an electrical low-pressure impactor (ELPI). We evaluated the particle size and composition distributions of 16 priority PAHs, designated by the US Environmental Protection Agency (EPA), that were emitted from the exhaust of a 4-st/mc operated at three speeds. We then used the toxic equivalency factors (TEFs) proposed by Nisbet and LaGoy (1992)^[22] to estimate the health risk of particulate-bound PAHs.

Materials and methods

Motorcycle and testing

PM was sampled from the exhaust of a 4-stroke carburetor motorcycle. This one-cylinder motorcycle had a bore and stroke of 51 mm \times 60 mm, a total displacement of 125 cm³, a compression ratio of 10.1:1, a maximum power of 6.0 kW/7500 rpm, and a maximum torque of 0.85 kgm/6000 rpm. A carburetor was used for the fuel supply system. Commercial 95-octane unleaded fuel from the Chinese Petroleum Company was used as the test fuel. Based on Taiwan's metropolitan characteristics, topography, and regulations, these motorcycles can be driven only on local roads, not on the freeway. They are generally used for short-distance transport; during the rush hour, the average distance travelled and speed are ca. 5–8 km/trip and 30 km/h, respectively.^[23,24] The driving patterns of vehicles operated at three different cruising speeds (idling and 15 and 30 km/h) were applied in the tests. To enhance the PAH analytical sensitivity, each ELPI sampling was performed over 60 min and repeated three times.

ELPI

The number and size distributions of the particles were measured using an ELPI (Dekati, Ltd.) equipped with aluminum foil (diameter: 37 mm) to collect size-resolved aerosol samples. The instrument sampled air at a nominal flow rate of 10 L/min. The ELPI had three main components: a cascade impactor, a unipolar diode charger, and a multichannel electrometer; it was used to simultaneously measure the charges carried by the collected particles at each stage. The measured current signals were then converted to number concentrations based on the response function of the charger. The function relates the measured current to the number concentration at different particle

sizes. These impactors effectively separated the PM into 13 ranges (at 50% efficiency) with the following equivalent cut-off diameters: 0.03, 0.06, 0.09, 0.17, 0.26, 0.38, 0.65, 0.95, 1.61, 2.50, 4.40, 6.80, and 9.97 μm . Accordingly, the particles were divided into four size groups: nano ($0.03 \mu\text{m} \leq d_p < 0.09 \mu\text{m}$), ultrafine ($0.17 \mu\text{m} \leq d_p < 0.38 \mu\text{m}$), fine ($0.65 \mu\text{m} \leq d_p < 1.61 \mu\text{m}$), and coarse ($2.50 \mu\text{m} \leq d_p < 9.97 \mu\text{m}$). In this study, the combined filters were extracted together for PAH analysis. Combining the 12 filters into four groups increased the sensitivity of the PAH analysis.

PAH analysis

In this study, only particle-bound PAHs were analyzed. The combined filter samples were extracted using a mixed solvent [*n*-hexane (30 mL) and dichloromethane (30 mL)] under ultrasonication for 2 h. The extract was then concentrated to 2 mL by purging with ultra-pure N₂ for the cleanup procedure. A C₁₈ cartridge (500 mg, 6 mL, Supelco) was applied to the cleanup procedure; it was pre-conditioned using methanol (6 mL), dichloromethane (6 mL), and *n*-hexane (6 mL). After cleaning the cartridge, the eluted solutions were discarded. The 2-mL concentrated sample was then transferred onto the C₁₈ cartridge; the vessel's walls were rinsed *n*-hexane (2 \times 2 mL), and then the washings were also added to the cartridge. Next, *n*-hexane (18 mL) was added to the cartridge and allowed to flow through it at a rate of 0.1–0.5 mL/min. The collected eluate was re-concentrated to 0.5 mL under a stream of ultra-pure N₂ to complete the cleanup procedure. The concentrations of the following PAHs were determined: naphthalene (Nap), acenaphthylene (Acpy), acenaphthene (Acp), fluorine (FL), phenanthrene (PA), anthracene (Ant), fluoranthene (Flu), pyrene (pyr), benz[a]anthracene (BaA), chrysene (CHR), benzo[b]fluoranthene (BbF), benzo[k]fluoranthene (BkF), benzo[a]pyrene (BaP), indeno[1,2,3-*cd*]pyrene (IND), dibenz[a,h]-anthracene (DBA), and benzo[ghi]perylene (Bghip).

PAHs were identified and quantified using an Agilent 6890 gas chromatograph equipped with an Agilent 5973N mass-selective detector (MS); a computer workstation was used for the PAH analysis. This gas chromatography/mass spectrometry (GC/MS) system was equipped with an Abel Bonded capillary column featuring a polysiloxane stationary phase (50 m \times 0.32 mm \times 0.17 μm); the film thickness injection volume was 1 μL ; splitless injection was performed at 310°C; the ion source temperature was 290°C; the oven temperature was increased from 50 to 100°C at 20°C/min, from 100 to 290°C at 3°C/min, and then held at 290°C for 40 min. The masses of the primary and secondary ions of the PAHs were determined using the scan mode for pure PAH standards. In this study, two internal standards (phenanthrene-*d*₁₀ and perylene-*d*₁₂) were used to check the response factors and the recovery efficiencies for the PAH analyses.^[25,26] The recovery efficiencies of 16 individual PAHs and 2 internal standards were determined

Table 1. Recovery efficiencies of *p*-PAH species.

PAH	Recovery efficiency (%)
Nap	87.6 ± 1.38
AcPy	88.0 ± 4.56
Acp	87.4 ± 12.4
Flu	87.3 ± 21.2
PA	85.8 ± 9.15
Ant	85.9 ± 10.6
FL	85.4 ± 19.4
Pyr	85.5 ± 11.8
BaA	85.2 ± 7.46
CHR	87.7 ± 17.7
BbF	82.2 ± 18.6
BkF	88.5 ± 15.0
BaP	86.9 ± 11.5
IND	82.7 ± 17.0
DBA	85.3 ± 4.51
BghiP	86.7 ± 0.72

directly after their addition to the filter samples. All of these spiked samples, containing known PAH concentrations (1 ppm), were subjected to the same extraction, concentration, and clean-up procedures mentioned above. The recovery efficiencies of the PAH standards (from 85.5 ± 11.8% to 88.5 ± 15.0%) were fairly constant (Table 1).

Method detection limits (MDLs) are defined as the minimum concentrations of the target analytcs that could be measured and reported with 99% confidence that the concentration was greater than zero; they were determined using standard procedures.^[27] Prior to analysis, calibration curves of the 16 PAHs were developed such that their values of R^2 were greater than 0.995 for analyzing PAH samples. MDLs were determined using a PAHs standard (10 ppb), i.e., at a concentration slightly higher than the lowest concentration of the calibration curve.

The standard deviation was estimated after repeating this process 7 times; the MDL was considered to be equal to three times the standard deviation. Recovery tests were performed with at least 10% of the samples being analyzed

after spiking with various amounts of the PAHs. The MDLs of the 16 PAHs analyzed were as follows: Nap, 0.74 ng; AcPy, 0.41 ng; Acp, 0.32 ng; Flu, 0.12 ng; PA, 0.06 ng; Ant, 0.09 ng; FL, 0.19 ng; Pyr, 0.57 ng; BaA, 0.02 ng; CHR, 0.09 ng; BbF, 0.14 ng; BkF, 0.04 ng; BaP, 0.02 ng; IND, 0.07 ng; DBA, 0.15 ng; BghiP, 0.06 ng.

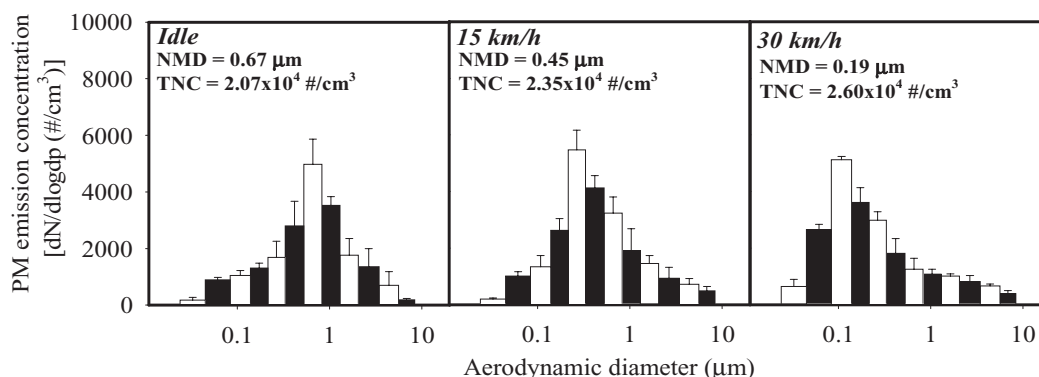
Carcinogenic potency

The carcinogenic potency of a given PAH can be expressed in terms of the BaP emission equivalent (BaP_{eq}), which is the product of its toxic equivalency factor (TEF)^[21] and its concentration. The TEF reflects the actual state of knowledge on the toxic potency of each individual PAH. The carcinogenic potency of the total-PAHs (total- BaP_{eq}) was the sum of the BaP emission equivalents of the 16 individual PAHs.

Results and discussion

Number distribution of particulate matter in motorcycle exhaust

The load and speed of a motorcycle affect both the size and number of its exhaust particles. Figure 1 presents the particle number concentrations ($\#/cm^3$) and size distributions ($dN/d\log d_p$ versus d_p) of the particles emitted from the 4-st/mc when operated at 3 different speeds. When idling and at 15 and 30 km/h, the total number concentrations (TNCs) were 2.07×10^4 , 2.35×10^4 , and $2.60 \times 10^4 \#/cm^3$, respectively. We applied a 1-sample *t*-test to identify significant differences between the TNCs of the particles emitted at the 3 speeds. This statistical analysis also revealed that the number concentrations at 15 ($p = 0.03$) and 30 ($p = 0.04$) km/h were significantly higher than that at idle (significance level: $\alpha = 0.05$). The particle number concentration increased upon increasing the speed. In general, at high vehicular speeds, the particle number concentration increases because of a higher engine load, exhaust temperature, or exhaust flow, resulting in greater TNCs at high speeds.^[28,29]

**Fig. 1.** Number and size distributions of PM emitted from a 4-st/mc operated at idle and at 15 and 30 km/h.

Our findings are similar to those reported for diesel and gasoline vehicles.^[30–34]

Figure 1 also presents the size distributions of the particles at idle and at speeds of 15 and 30 km/h. Approximately 80% of the particles emitted from the motorcycle were smaller than 1.0 μm , indicating that they were primary inhalable particulates. Notably, however, the particle size distributions at the three speeds were significantly different. When idling, fine particulates were the major component. After increasing the speed to 15 km/h, the level of ultra-fine particulates increased; at 30 km/h, nano-particulates predominated the size distribution.

The number-median diameter (NMDs) of a particulate matter can be determined from the plot of its cumulative fractions; the value is equal to the particle diameter at 50% in the cumulative curve. The NMDs of the particles at idle and at 15 and 30 km/h were 0.67, 0.45, and 0.19 μm , respectively. Our results indicate that smaller particles gradually dominated in the exhaust upon increasing the speed of the 4-st/mc. Although, the TNCs of the particles emitted at higher speeds were greater, most of them were smaller particles. Thus, we suspect that the more-complete combustion of fuel at higher speeds may have led to the decrement of larger particulates.

Concentration of PAHs in the four particle-size ranges

Figure 2 displays the emission concentrations of the 16 PAHs in the four particle-size ranges at each of the three speeds of operation. At idle and at 15 and 30 km/h, the total-PAH (t-PAH) emission concentrations were 339, 243, and 220 ng/m^3 , respectively. Generally, a higher combustion efficiency, which is often associated with a higher combustion temperature, occurs at higher speeds.^[29,35,36] Such a phenomenon might explain why the values of t-PAH decreased at greater engine speeds.

Although the trends of the total PAHs and the total number concentrations at the three speeds were contrasting, the t-PAH distributions in the different particle-size ranges (Fig. 2) were quite similar to the corresponding number distributions of particles (Fig. 1); i.e., the higher concen-

tration of t-PAHs shifted to finer particulate size ranges as the engine speed increased. Such results are expected because emissions of particle-bound PAHs are highly related to those of PM. At idle and at 15 and 30 km/h, the mass percentages of PAHs in the PM were 31.0, 33.9, and 26.6%, respectively, in the ultra-fine-size range and 15, 21.5, and 40.9%, respectively, in the nano-range. Thus, higher percentages of PAHs were contained in the ultra-fine and nano-particulate ranges for the exhaust gases emitted at higher speeds. Note that particle-bound PAHs may exhibit enhanced toxicity and pose greater harm to human health when associated with ultra-fine and nano-sized particles.

PAH

PAHs are generally derived from the unburned (or incompletely burned) pyrolysis and/or pyrosynthesis condensation of fuel and lubricant oil.^[37,38] The composition of the fuel plays an important role in determining the PAH emission from engine combustion.^[4,9,12,38,39] Table 1 lists the main PAH species present in 95-octane unleaded fuel. The scope of the concentrations of these PAHs is widespread (from 0.001 to 206 ppm). Most of the PAHs present in this fuel are low-molecular-weight compounds. The concentration ranges of the top three PAHs—Nap, PA, and Ant—were 147–206, 25.8–36.5, and 17.9–24.5 ppm, respectively. Figure 3 presents the percentages of the 16 PAHs contained in the 4 size-group ranges (nano, ultra-fine, fine and coarse) of the particles exhausted from the 4-st/mc operated at the 3 speeds. The principal PAH species were the three-ring compounds PA and Ant, followed by Pyr, CHR, BaP, IND, and DBA.

The major PAH species contained in the four particle-size ranges varied at each speed. Figure 3 reveals that lower-molecular-weight (Acp, Flu, PA, Ant, Pyr, CHR) and 5-ring (BaP, IND, DBA) PAHs were the main emission species when idling. It seems that, excluding the incomplete combustion of fuel, some of the lower-molecular-weight PAHs (e.g., PA, Ant, Pyr), which existed at notably higher levels in the fine particles, may have originated from unburned 95-octane unleaded fuel. In contrast, the presence of

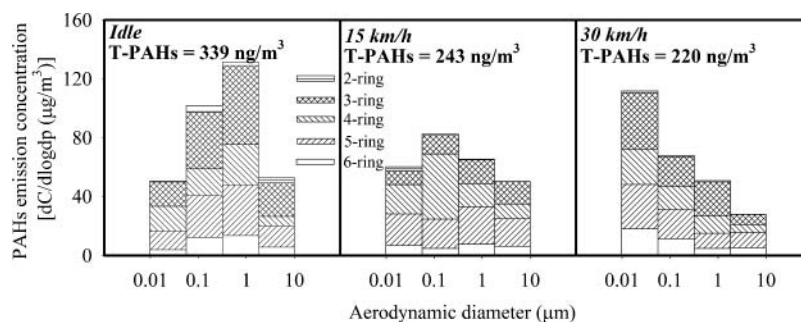


Fig. 2. Concentration distributions of PAHs in the 4 size ranges of the PM emitted from a 4-st/mc operated at idle and at 15 and 30 km/h.

Table 2. Concentrations of the 16 main PAH species present in the 95-unleaded fuel.

PAH	Range (ppm)	Mean \pm standard deviation	Percentage (%)
Nap	147–206	176 \pm 10.6	68.8
AcPy	8.00–18.3	13.1 \pm 3.87	5.13
Acp	0.061–0.304	0.183 \pm 0.62	0.07
Flu	1.83–3.24	2.53 \pm 0.29	0.99
PA	25.8–36.5	31.1 \pm 1.83	12.1
Ant	17.9–24.5	21.2 \pm 1.67	8.27
FL	2.38–2.93	2.66 \pm 0.12	1.04
Pyr	5.02–6.02	5.52 \pm 0.92	2.15
BaA	1.86–2.51	2.18 \pm 0.23	0.57
CHR	0.489–1.021	0.750 \pm 0.04	0.29
BbF	0.010–0.021	0.016 \pm 0.04	0.01
BkF	0.014–0.022	0.018 \pm 0.02	0.01
BaP	0.490–2.057	1.274 \pm 0.07	0.50
IND	0.001–0.010	0.006 \pm 0.11	0.002
DBA	0.002–0.003	0.002 \pm 0.17	0.001
BghiP	0.002–0.004	0.003 \pm 0.11	0.001

higher-molecular-weight PAHs, which are found at lower levels in the fuel, may have originated from other sources, such as the lubricating oil or through pyrosynthesis.^[7,9,33]

After increasing the driving speed to 15 km/h, the main PAHs species were Ant, Pyr, CHR, BaP, and IND. Most of these compounds were present in the ultrafine particles. Relative to the idle mode, the levels of the medium-molecular-weight PAHs (FL, Pyr, BaA, CHR) increased in the ultrafine particles, whereas those of the small (PA, Ant) and large (BaP, DBA) PAHs decreased. Because elevating the driving speed can lead to more-complete combustion efficiency,^[25,30] we suspect that pyrolysis of the PAHs might have occurred, thereby leading to increases in the levels of the mid-sized products.

When the speed of the 4-st/mc was 30 km/h, more of the pyrosynthesis products (BaP, IND, DBA) were induced through the corresponding higher-temperature com-

bustion. Notably, most of the particles exhausted at that speed were nanoparticles (Fig. 1). We suspect that condensation of the PAHs as nuclei might have predominated, thereby leading to most of the PAHs being contained in the nanoparticles (Fig. 2).

BaP-equivalent carcinogenicity of particles of various sizes in motorcycle exhaust emission

In this study, we applied TEFs to assess the carcinogenic potencies of the 16 analyzed PAHs in the nano, ultrafine, fine, and coarse particulates emitted at the 3 speeds. We developed these TEFs as a means of comparing the carcinogenic potencies of the individual PAHs relative to the carcinogenicity of BaP. Each TEF is expressed in terms of its BaP emission equivalent (BaP_{eq}). We calculated the BaP_{eq} factor for each individual PAH by multiplying its emission concentration by its corresponding TEF. The total-BaP_{eq} (t-BaP_{eq}) emission concentrations in the four size ranges of the particles emitted at idle and at 15 and 30 km/h were 15.3, 11.8, and 11.6 $\mu\text{g}/\text{m}^3$, respectively (Fig. 4). Indeed, the t-BaP_{eq} emission concentrations for all particle-size ranges when idling were higher than those at the other 2 speeds.

As the engine speed increased, the total BaP_{eq} emission concentration decreased accordingly. Notably, however, when compared with Figure 2, the t-BaP_{eq} emissions were inconsistent with the total PAH emissions, especially for the ultrafine particles emitted at 15 km/h and for the coarse particles emitted at 30 km/h. In terms of carcinogenicity, we suspect that the 5- (BaP, DBA) and 6-ring (IND) PAHs are probably the main sources of carcinogenicity in the emissions from the 4-st/mc. The main PAHs emitted in the ultrafine particles at 15 km/h were four-ring compounds, which are less carcinogenic.

In contrast, the main PAH species emitted in the coarse particles at 30 km/h were 5- and 6-ring compounds, which are more carcinogenic. In summary, although the total PAH concentration is an important factor when determining the carcinogenicity of PAHs, the nature of

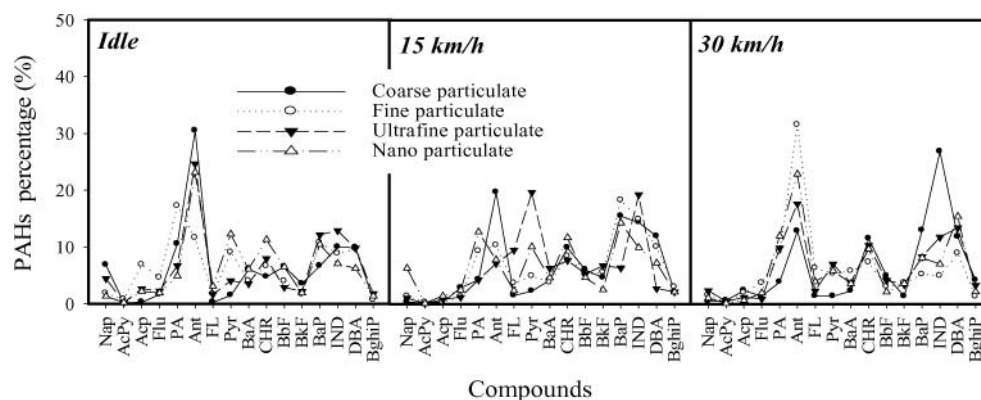


Fig. 3. PAH compounds in the 4 groups of size ranges (nano, ultrafine, fine, coarse) of the PM emitted from a 4-st/mc operated at idle and at 15 and 30 km/h.

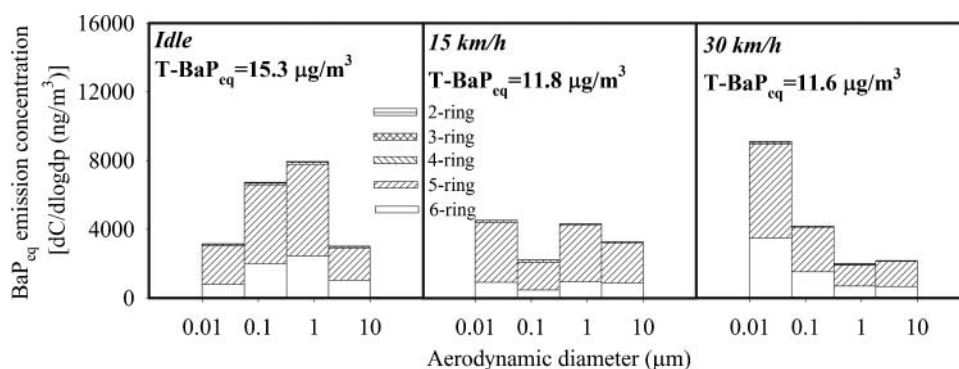


Fig. 4. BaP_{eq} emission concentrations in the 4 groups of size ranges of the PM emitted from a 4-st/mc operated at idle and at 15 and 30 km/h.

the individual PAH species should also be taken into consideration.

Conclusion

In this study, we examined the effects of three different speeds (idling, 15 km/h, 30 km/h) on the particulate sizes, particle size distributions of PAHs, and carcinogenic potencies of the emissions from a 4-st/mc. Although the TNC of the particles increased upon increasing the engine speed, smaller particles became more prominent accordingly. Both the t-PAH emission concentration and the PAH corresponding carcinogenic potency over the entire particle size range decreased in the exhaust gas upon increasing the speed, which also caused a higher proportion of the PAHs to be contained in ultra-fine and nano-sized particulates. The particulates that were emitted in the nano size range from the 4-st/mc at higher speeds had the strongest PAH-related carcinogenic potencies; this particle size range might be the greatest vector for transferring various carcinogenic compounds into the human body.

References

- [1] Lin, C.W.; Chen, Y.R.; Lu, S.J.; Cho, S.W.; Lin, K.S.; Chiu, Y.C.; Tang, X.Y. Relationships between characteristics of motorcycles and hydrocarbon emissions in Taiwan: A note. *Transp. Res.* **2008**, *13*, 351–354.
- [2] Tsai, J.H.; Hsu, Y.C.; Weng, H.C.; Lin, W.Y.; Jeng, F.T. Air pollutant emission factors from new and in-use motorcycles. *Atmos. Environ.* **2000**, *28*, 4747–4754.
- [3] Yang, H.H.; Hsieh, L.T.; Liu, H.C.; Mi, H.H. Polycyclic aromatic hydrocarbon emissions from motorcycles. *Atmos. Environ.* **2005**, *39*, 17–25.
- [4] Yao, Y.C.; Tsai, J.H.; Chang, A.L.; Jeng, F.T. Effects of sulfur and aromatic contents in gasoline on motorcycle emissions. *Atmos. Environ.* **2008**, *42*, 6560–6564.
- [5] Mukherji, S.; Swain, A.K.; Venkataraman, C. Comparative mutagenicity assessment of aerosols in emissions from biofuel combustion. *Atmos. Environ.* **2002**, *36*, 5627–5635.
- [6] Kawanaka, Y.; Matsumoto, E.; Sakamoto, K.; Wang, N.; Yun, S.J. Size distributions of mutagenic compounds and mutagenicity in atmospheric particulate matter collected with a low-pressure cascade impactor. *Atmos. Environ.* **2004**, *14*, 2125–2132.
- [7] Mastral, A.M.; Callén, M.S. A review on polycyclic aromatic hydrocarbon (PAH) emissions from energy generation. *Environ. Sci. Technol.* **2000**, *34*, 3051–3057.
- [8] Larsen, R.K.; Baker, J.E. Source apportionment of polycyclic aromatic hydrocarbons in the urban atmosphere: A comparison of three methods. *Environ. Sci. Technol.* **2003**, *37*, 1873–1881.
- [9] Lim, M.C.H.; Ayoko, G.A.; Morawska, L.; Ristovski, Z.D.; Jayaratne, E.R. Influence of fuel composition on polycyclic aromatic hydrocarbon emissions from a fleet of in-service passenger cars. *Atmos. Environ.* **2007**, *41*, 150–160.
- [10] Westerholm, R.N.; Almén, J.H.; Rannug, J.U.; Egeback, K.E.; Grägg, K. Chemical and biological characterization of particulate-, semivolatile-, and gas-phase-associated compounds in diluted heavy-duty diesel exhausts: A comparison of three different semivolatile-phase samplers. *Environ. Sci. Technol.* **1991**, *25*, 332–338.
- [11] Yang, H.H.; Chien, S.M.; Chao, M.R.; Lin, C.C. Particle size distribution of polycyclic aromatic hydrocarbons in motorcycle exhaust emissions. *J. Hazard. Mater.* **2005**, *125*, 154–159.
- [12] Spezzano, P.; Picini, P.; Cataldi, D. Gas- and particle-phase distribution of polycyclic aromatic hydrocarbons in two-stroke, 50-cm³ moped emissions. *Atmos. Environ.* **2008**, *43*, 539–545.
- [13] Chan, C.C.; Nien, C.K.; Tsai, C.Y.; Her, G.R. Comparison of tail-pipe emissions from motorcycles and passenger cars. *J. Air Waste Manage. Assoc.* **1995**, *45*, 116–124.
- [14] Tsai, J.H.; Chiang, H.L.; Hsu, Y.C.; Weng, H.C.; Yang, C.Y. The speciation of volatile organic compounds (VOCs) from motorcycle engine exhaust at different driving modes. *Atmos. Environ.* **2003**, *37*, 2485–2496.
- [15] Leong, S.T.; Muttamara, S.; Laortanakul, P. Influence of benzene emission from motorcycles on Bangkok air quality. *Atmos. Environ.* **2000**, *36*, 651–661.
- [16] Chang, C.T.; Chen, B.Y. Toxicity assessment of volatile organic compounds and polycyclic aromatic hydrocarbons in motorcycle exhaust. *J. Hazard. Mater.* **2008**, *153*, 1262–1269.
- [17] Kleeman, M.J.; Schauer, J.J.; Gass, G.R. Size and composition distribution of fine particulate matter emitted from motor vehicles. *Environ. Sci. Technol.* **2000**, *34*, 1132–1142.
- [18] Zielinska, B.; Sagerbiel, J.; Arnott, W.P.; Roggers, C.F.; Kelly, K.E.; Wagner, D.A.; Lighty, J.S.; Sarofim, A.F.; Palmer, G. Phase and size distribution of polycyclic aromatic hydrocarbons in diesel and gasoline vehicle emissions. *Environ. Sci. Technol.* **2004**, *38*, 2557–2567.

- [19] Beddowsa C.S.D.; Harrison, R. M. Comparison of average particle number emission factors for heavy and light duty vehicles derived from rolling chassis dynamometer and field studies. *Atmos. Environ.* **2008**, *42*, 7954–7966.
- [20] Lin, C.C.; Chen, S.J. Huang, K.L. Hwang, W.I. Chang-Chien, G.P. Lin, W.Y. Characteristics of metals in nano/ultrafine/fine/coarse particles collected beside a heavily trafficked road. *Environ. Sci. Technol.* **2005**, *39*, 8113–8122.
- [21] Lin, C.C. Chen, S.J. Huang, K.L. Lee, W.J. Lin, W.Y. Tsai, J.H. Chaung H.C. PAHs, PAH-induced carcinogenic potency, and particle-extract-induced cytotoxicity of traffic-related nano/ultrafine particles. *Environ. Sci. Technol.* **2008**, *42*, 4229–4235.
- [22] Nisbet, I.C.T.; LaGoy, P.K. Toxic equivalency factors (TEFs) for polycyclic aromatic hydrocarbons (PAHs). *Regul. Toxicol. Pharm.* **1992**, *16*, 290–300.
- [23] Chen, K.S.; Wang, W.C.; Chen, H.M.; Lin, C.F.; Hsu, H.C.; Kao, J.H.; Hu, M.T. Motorcycle emissions and fuel consumption in urban and rural driving conditions. *Sci. Total Environ.* **2003**, *312*, 113–122.
- [24] Tsai, J.H.; Chiang, H.L.; Hsu, Y.C.; Peng, B.J.; Hung, R.F. Development of a local real world driving cycle for motorcycles for emission factor measurements. *Atmos. Environ.* **2005**, *39*, 631–664.
- [25] Yang, H.H.; Chien, S.M., Cheng M.T.; Peng, C.Y. Comparative study of regulated and unregulated air pollutant emissions before and after conversion of automobiles from gasoline power to liquefied petroleum gas/gasoline dual-fuel retrofits. *Environ. Sci. Technol.* **2007**, *41*, 8471–8476.
- [26] Kawanaka, Y.; Yoshiteru, T.; Yun S.J.; Sakamoto, K. Size distributions of polycyclic aromatic hydrocarbons in the atmosphere and estimation of the contribution of ultrafine particles to their lung deposition. *Environ. Sci. Technol.* **2009**, *43*, 6851–6856.
- [27] EPA, 1996. Chapter 1 Quality Control, Test Methods for Evaluating Solid Waste, Physical/Chemical Methods, EPA SW-846, Revision 3. US Environmental Protection Agency. Available from: <<http://www.epa.gov/epawaste/hazard/testmethods/index.htm>>.
- [28] Giechaskiel, B.; Ntziachristos, L.; Samaras, Z.; Scheer, V.; Casati, R.; Vogt, R. Formation potential of vehicle exhaust nucleation mode particles on-road and in the laboratory. *Atmos. Environ.* **2005**, *39*, 3191–3198.
- [29] Desantes, J.M.; Bermúdez, V.; García, J.M.; Fuentes, E. Effects of current engine strategies on the exhaust aerosol particle size distribution from a heavy-duty diesel engine. *J. Aerosol Sci.* **2005**, *36*, 1251–1276.
- [30] Kittelson, D.B.; Watts, W.F.; Johnson, J.P. Nanoparticle emissions on Minnesota highways. *Atmos. Environ.* **2004**, *38*, 9–19.
- [31] Annele, K.K.; Virtanen, J.M.R.; Kati, M.V.; Jorma, K. Effect of engine load on diesel soot particles. *Environ. Sci. Technol.* **2004**, *38*, 2551–2556.
- [32] Li, X.L.; Huang, Z.; Wang J.S.; Zhang, W.G. Particle size distribution from a GTL engine. *Sci. Total Environ.* **2007**, *382*, 295–303.
- [33] Riddle, S.G.; Robert, M.A.; Jakober, C.A.; Hannigan M.P.; Klee-man, M.J. Size distribution of trace organic species emitted from heavy-duty diesel vehicles. *Environ. Sci. Technol.* **2007**, *41*, 1962–1969.
- [34] Chen, K.S.; Wang, H.K.; Wang W.C.; Lai, C.H. Measurement and receptor modeling of atmospheric polycyclic aromatic hydrocarbons in urban Kaohsiung, Taiwan. *J. Hazard. Mater.* **2009**, *166*, 873–879.
- [35] Cooper, D.A. Exhaust emissions from high speed passenger ferries. *Atmos. Environ.* **2001**, *35*, 4189–4200.
- [36] Tancell, P.J.; Rhead, M.M.; Pemberton R.D.; Braven, J. Survival of polycyclic aromatic hydrocarbons during diesel combustion. *Environ. Sci. Technol.* **1995**, *29*, 2871–2876.
- [37] Miguel, A.H.; Kirchstetter, T.W.; Harley, R.A. On-rad emissions of particulate polycyclic aromatic hydrocarbons and black carbon from gasoline and diesel vehicle. *Environ. Sci. Technol.* **1998**, *32*, 450–455.
- [38] Marr, L.C.; Kirchstetter, T.W.; Harley, R.A.; Miguel, A.H.; Hering S.V.; Hammond, S.K. Characterization of polycyclic aromatic hydrocarbons in motor vehicle fuels and exhaust emissions. *Environ. Sci. Technol.* **1999**, *33*, 3091–3099.
- [39] Jia, L.W.; Zhou, W.L.; Shen, M.Q.; Wang, J.; Lin, M.Q. The investigation of emission characteristics and carbon deposition over motorcycle monolith catalytic converter using different fuels. *Atmos. Environ.* **2006**, *40*, 2002–2010.